AFRL-RH-BR-TR-2007-0065

Numerical Modeling of Antenna Near Field

Dr. Surendra Singh
Dr. William P. Roach

Air Force Research Laboratory

August 2007

Approved for Public Release - 07-333, 15 Oct 2007

Air Force Research Laboratory
Human Effectiveness Directorate
Directed Energy Bioeffects Division
Radiofrequency Radiation Branch
Brooks-City-Base, TX 78235

NOTICE AND SIGNATURE PAGE

AFRL-RH-BR-TR-2007-0065 HAS BEEN REVIEWED AND IS APPROVED FOR PUBLICATION IN ACCORDANCE WITH ASSIGNED DISTRIBUTION STATEMENT.

______//SIGNED//________________________
NOEL D MONTGOMERY, LtCol, USAF
Program Manager

______//SIGNED//________________________
GARRETT D POLHAMUS, DR-IV, DAF
Chief, Directed Energy Bioeffects Division

REPORT DOCUMENTATION PAGE	*Form Approved* *OMB No. 0704-0188*

1. REPORT DATE *(DD-MM-YYYY)*	**2. REPORT TYPE**	**3. DATES COVERED** *(From - To)*
10 August 2007	**Technical Report**	May-August 2007

4. TITLE AND SUBTITLE Numerical Modeling of Antenna Near Field	**5a. CONTRACT NUMBER** N/A **5b. GRANT NUMBER** N/A **5c. PROGRAM ELEMENT NUMBER** 62202F
6. AUTHOR(S) Dr Surendra Singh and Dr William P. Roach	**5d. PROJECT NUMBER** 7757 **5e. TASK NUMBER** B3 **5f. WORK UNIT NUMBER** 48
7. PERFORMING ORGANIZATION NAME(S) AND ADDRESS(ES) Human Effectiveness Directorate, Directed Energy Bioeffects Division, Radio Frequency Radiation Branch 8262 Hawks Road Brooks City-Base, TX 78235	**8. PERFORMING ORGANIZATION REPORT NUMBER**
9. SPONSORING / MONITORING AGENCY NAME(S) AND ADDRESS(ES) Air Force Materiel Command Air Force Research Laboratory Human Effectiveness Directorate Directed Energy Bioeffects Division Radio Frequency Radiation Branch 8262 Hawks Road Brooks City-Base, TX 78235	**10. SPONSOR/MONITOR'S ACRONYM(S)** AFRL/RHDR **11. SPONSOR/MONITOR'S REPORT NUMBER(S)** **AFRL-RH-BR-TR-2007-0065**

12. DISTRIBUTION / AVAILABILITY STATEMENT
Distribution A. For Public Release, 07-333, 15 October 2007

13. SUPPLEMENTARY NOTES
N/A

14. ABSTRACT
This work provides numerical modeling for the near field of a wire antenna. The conventional near field definition is provided along with an explanation for the maximum power density in the near field. Numerical results are provided for the electric and magnetic fields in the near field region. The results obtained from the model are shown to compare very well with data available in the literature for the thin wire case. The variation of the wave impedance and power density are also studied. A listing of the code developed in MATLAB is included in an appendix.

15. SUBJECT TERMS

Near field, Antenna, Power Density, Far Field

16. SECURITY CLASSIFICATION OF:			**b. ABSTRACT**	**18. NUMBER OF PAGES**	**19a. NAME OF RESPONSIBLE PERSON**
					William P Roach, USAF
a. REPORT U	**Standard Form 298 (Rev. 8-98)** **U**	**c. THIS PAGE** Unclass	Unclass	44	**19b. TELEPHONE NUMBER** *(include area code)*

TABLE OF CONTENTS

PAGE

LIST OF FIGURES

EXECUTIVE SUMMARY

This work provides numerical modeling of the near field of a wire antenna. The conventional near field definition is derived along with the analytic expression for the power density in the near field. The study is motivated by the fact that the electric and magnetic fields in the near field region may pose a radiation hazard due to higher than expected field values. With accurate modeling of the near fields, it will be possible to identify and predict such hazards. Numerical results are provided for the electric and magnetic fields in the near field region of a thin wire antenna. The results obtained from the model are shown to compare very well with data available in the literature for the thin wire case. The variation of the wave impedance and power density are also studied. It is determined that the wave impedance goes through very sharp changes in the near field region and that it approaches the free space value as the far field region is approached. A similar behavior is observed for the power density as well. The next step in the study will be to consider the impact of the near field excitation on a dielectric body. The heating effect in the dielectric body due to the near field will provide insight into the impact of the near field in comparison to a plane wave excitation. The work can also be extended to consider the near field of other antenna geometries of interest. For convenience, the computer code developed in MATLAB is provided in the appendix.

1.0 INTRODUCTION

The objective of this work is to develop a computational model to accurately predict the near field of an antenna. As a starting point and for the sake of simplicity, a thin wire antenna is considered. After modeling the near field for this antenna and understanding the mechanics of the associated near field, more complex antenna configurations, such as a parabolic dish antenna will be attempted as a continuation of this work. To give a simple definition for the near field, as the name suggests, it is the field very close to the antenna. A more rigorous definition is provided in the next section. The nature of the near field is quite complex. As a result, very few antenna geometries have been studied in detail. Most often the models make assumptions to simplify the mathematical analysis and modeling. Thereby, leaving the true nature of the near field relatively unknown. An accurate description of the near field is necessary because of its' potential health hazard. This is due to the fact that in the near field region, the intensity of the field and consequently the resulting power density can exceed the recommended safety level. The radiation safety level given by the Federal Communications Commission (FCC) is 5 mW/cm^2 for controlled exposure and 1mW/cm^2 for general population in the frequency range from 1.5 GHz to 100 GHz [1]. The safety regulation by OSHA limits the power density to 10 mW/cm^2 when spatially averaged over a 6 minute period. Experimental work has demonstrated that the effect of radiofrequency (RF) radiation on living tissue is primarily in producing heat. This heating is a function of the strength of the RF radiation as well as the duration of exposure. The depth of penetration of the heat depends on the frequency of the radiation. Radiation at lower frequencies (200 MHz to 900 MHz) penetrates deeply whereas radiation at much higher frequencies (1.5 GHz and up) typically used by radars produce heating effects at or near the surface. The human body is capable of diffusing a portion of the heat as circulating blood in the body acts as a coolant. But, body organs which have little blood flow, such as eyes are particularly at risk [2]. Other risks from high levels of RF radiation include ignition of fuel. Electromagnetic energy is capable of inducing currents into any metallic object. This means that many parts of an aircraft and refueling vehicles may act as receiving antennas and create large enough power density to cause a spark and ignite fuel. To prevent such a potential hazard, a safety criterion of 5 W/cm^2 has been established for refueling operations [3].

2.0 DEFINITION OF NEAR FIELD

In this section, a precise definition of the near field in terms of the distance from the antenna is provided. Traditionally, textbooks in antenna theory define the near field to be the region surrounding the antenna such that $kr \ll 1$, where k is the propagation constant (or wave number of the medium) and r is the radial distance from the origin. An alternate definition, which defines the beginning of the far field region (also known as Fraunhofer region) is derived as follows [4]. Consider a filament of current along the z-axis and located near the origin as shown in the Fig. 1.

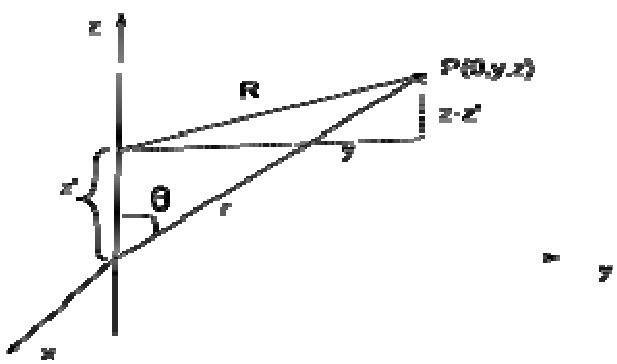

Figure 1: Field calculation for a filament of current source along the z-axis.

The magnetic vector potential, A_z, due to the current distribution on the filament, $I(z)$, is given by

$$A_z = \int I(z') \frac{e^{-jkr}}{4\pi R} dz' \tag{1}$$

where $R = |\vec{r} - \vec{r}'|$ represents the distance between the observation or field point (located by the position vector $\vec{r}$) and the source point (located by the position vector $\vec{r}'$). Since A_z is independent of the angular variation, ϕ, the vector potential can be evaluated in the $y - z$ plane , that is, for $\phi = 90^\circ$, yielding

$\vec{r} = y\hat{y} + z\hat{z},\ \vec{r}' = z'\hat{z}$ and $R = |\vec{r} - \vec{r}| = \sqrt{y^2 + (z - z')^2}$. Converting rectangular to spherical coordinates, $y = r\sin\theta,$ and $z = r\cos\theta,$ R can be written as

$$R = \sqrt{r^2 + z'^2 - 2rz'\cos\theta}$$

$$R = r\{1 + \frac{1}{r^2}(z'^2 - 2rz'\cos\theta)\}^{1/2}$$

The above expression for R can be expanded using Binomial theorem expansion as

$$R = r\left(1 + \frac{1}{2r^2}(z'^2 - 2rz'\cos\theta) - \frac{z'^2}{2r^2}\cos^2\theta + \text{terms of order}\left(\frac{1}{r^3}\right) + \ldots\right)$$

$$= r - z'\cos\theta + \frac{1}{2r}z'^2(1 - \cos^2\theta) + \ldots$$

$$= r - z'\cos\theta + \frac{1}{2r}z'^2\sin^2\theta + \ldots \tag{3}$$

In the integral given by Equation (1), the factor, R, in the denominator can be approximated by $R \approx r$. However, in the phase term, more accuracy is required and the proper approximation is

$$R \approx r - z'\cos\theta \tag{4}$$

This approximation is illustrated in Figure 2 as rays are drawn from each point on the source as parallel lines. The parallel ray assumption is exact only when the observation point is at infinity, but it is a good approximation in the far field. The definition of the distance from the source where the far field begins is taken to be where the parallel ray approximation begins to breakdown. The distance where the far field begins, r_{ff} is the value of r for which the path length deviation due to neglecting the term $\frac{z'}{2r}\sin^2\theta$ in

Equation (3) is $\frac{\lambda}{16}$. This corresponds to a phase error of $\frac{2\pi}{\lambda}\frac{\lambda}{16} = \frac{\pi}{8}\, radians$. If D is the length of the line source, r_{ff} is found by equating the maximum value of $\frac{z'}{2r}\sin^2\theta$ equal to $\frac{\lambda}{16}$, that is,

$$\left|\frac{z'^2}{2r_{ff}}\sin^2\theta\right|_{\max} = \frac{\lambda}{16}.$$

This occurs for $z' = D/2$ and $\theta = 90^\circ$, yielding

$$r_{ff} = \frac{2D^2}{\lambda} \tag{5}$$

With the far field distance identified, the distance to the near field is taken to be half of this distance. Therefore, the extent of the near field, r_{nf}, is given by

$$r_{nf} = \frac{D^2}{\lambda} \tag{6}$$

The region between $\frac{D^2}{\lambda}$ and $\frac{2D^2}{\lambda}$ is termed as Fresnel region or intermediate near field region, as illustrated in Figure 3.

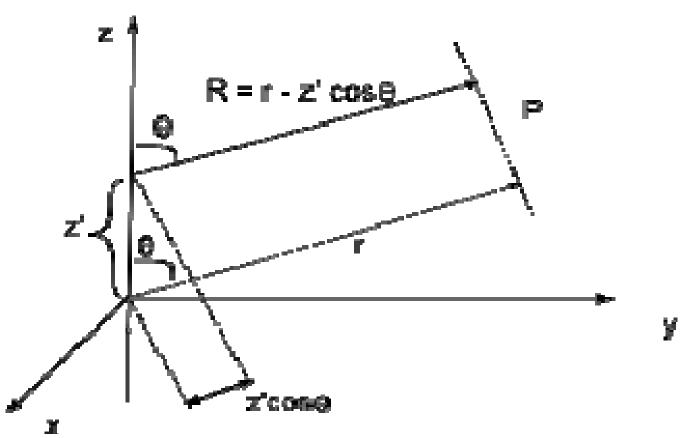

Figure 2: Parallel ray approximation for far field calculation of a filament of current.

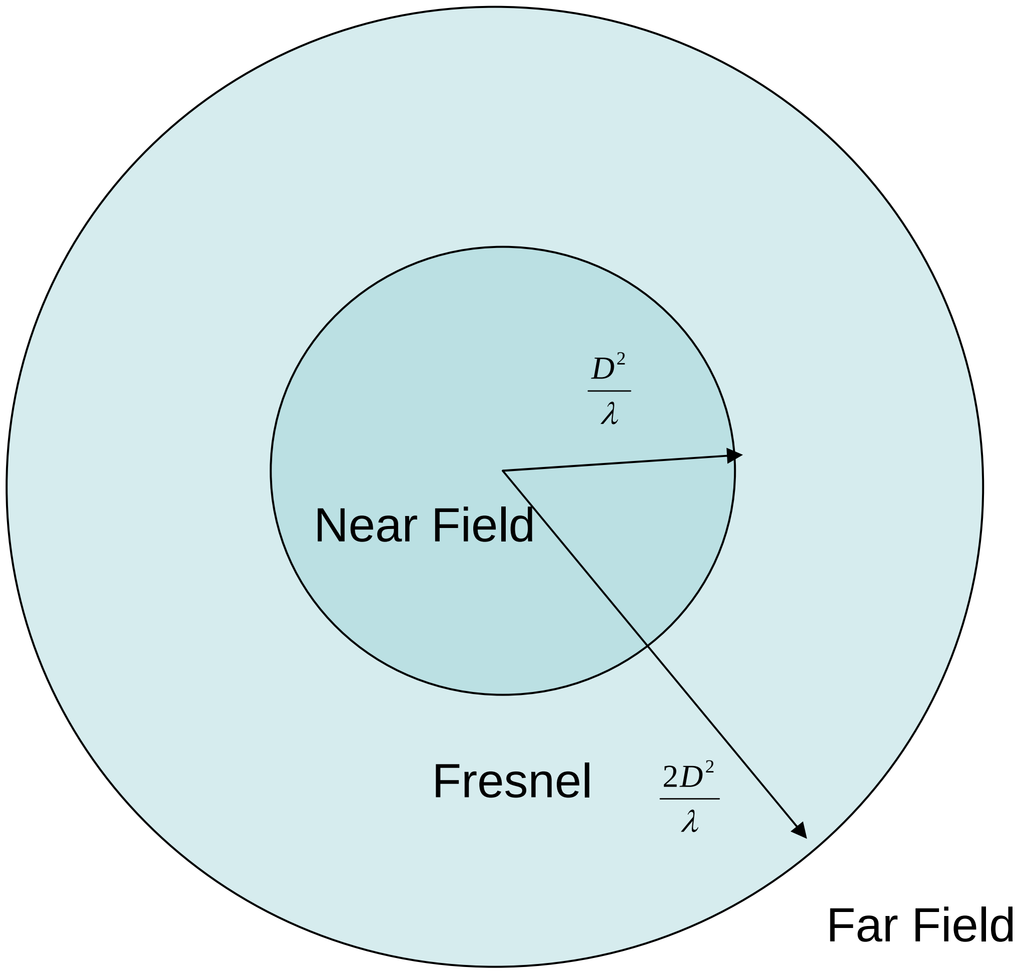

Figure 3: Near field and far field regions.

3.0 UPPER BOUND ON THE POWER DENSITY IN THE NEAR FIELD

As the power density in the near field defined by W, can exceed the power density at the antenna aperture defined by W_0, it is instructive to know the upper bound on W that has been established in the literature [2]. Consider an electromagnetic (EM) plane wave impinging on a totally absorbing body of area A. If the power density of the EM wave is W, then the power absorbed P is given by

$$P = WA \tag{7}$$

For an isotropic radiator in free space, radiating a total average power P in all directions equally, then the power density on the surface of a concentric sphere of radius r is given by

$$W = \frac{P}{A} = \frac{P}{4\pi\, r^2} \tag{8}$$

In case the radiator is not isotropic because it radiates with a directive gain $G(\theta, \phi)$ in a given direction, then the power density in the far field at a distance r will be

$$W = \frac{GP}{4\pi\, r^2} \tag{9}$$

A 100% ground reflection doubles the strength of the electric field and hence the power density gets quadrupled, That is

$$W = \frac{GP}{\pi\, r^2} \tag{10}$$

The antenna gain G can be written in terms of the antenna area as

$$G = \frac{4\pi\, A}{\lambda^2} \tag{11}$$

Substituting G from Eq (11) into Eq (9) gives the far field power density

$$W = \frac{AP}{\lambda^2 r^2} = \frac{W_0 A^2}{\lambda^2 r^2}$$

where $W_0 = P / A$ is the power density at the aperture. The above equation can be written as

$$\frac{W}{W_0} = \frac{A^2}{\lambda^2 r^2} \tag{12}$$

Similarly, substituting G from Eq (11) into Eq (10) gives the power density for the 100% reflection from the ground:

$$W = \frac{4AP}{\lambda^2 r^2} = \frac{4\, W_0 A^2}{\lambda^2 r^2}$$

or

$$\frac{W}{W_0} = 4\left(\frac{A^2}{\lambda^2 r^2}\right) \tag{13}$$

The expression in Eq (13) is valid in the far field region, but for a uniformly illuminated round aperture and in the limit $\left(\frac{A^2}{\lambda^2 r^2}\right) << 1$, the expression can be applicable in the near field region providing

$$\frac{W}{W_0} = 4\sin^2\left(\frac{A}{\lambda\, r}\right) \tag{14}$$

which has a maximum value of 4, thereby, providing the approximation for the near field as

$$W = 4W_0 \tag{15}$$

The power density of a reflector antenna can be shown to have a maximum envelop along the central axis of the antenna which is 6 dB (10 log4) above the average power density on the aperture up to a characteristic distance of $D^2/4\lambda$ and falls uniformly from that point on to the far field [5]. For instance, for a transmit power of about 3.6 kW from a 12 meter diameter aperture, the average power density is about 3.2 mW$/cm^2$, but could reach 12.8 mW$/cm^2$ along the central axis.

4.0 NEAR FIELD OF A WIRE ANTENNA

This section provides a mathematical formulation for computing the near field for a thin wire antenna. A formulation for solving an integral equation for the current distribution on the antenna element is presented. The resulting current distribution is then utilized in computing the electric and magnetic fields in the near field region. Consider an arbitrarily oriented as shown in Figure 4. The wire is assumed to be perfectly conducting. For thin wires, it is assumed that the wire radius is small compared to the wavelength and the length of the wire. The thin wire assumption allows the consideration of only axially directed currents. Therefore, there is no azimuth or circumferentially directed component of the current. The magnetic vector potential $\vec{A}$ and the electric scalar potential Φ are given by

$$\vec{A} = \frac{\mu}{4\pi}\int_c I(s')\,\hat{s}(s')\,k(s-s')\,ds' \tag{16}$$

and

$$\Phi = \frac{1}{4\pi\varepsilon}\int_c q(s')\,k(s-s')\,ds' \tag{17}$$

respectively, where

$$k(s-s') = \frac{1}{2\pi}\int_{-\pi}^{\pi}\frac{e^{-jkR}}{R}\,\mathrm{ds'} \tag{18}$$

$$R = \left((s-s')^2 + 4a^2\sin^2\frac{\phi}{2}\right)^{1/2} \tag{19}$$

$$q(s) = \frac{-1}{j\omega}\frac{d}{ds}I(s) \tag{20}$$

In the above equations, $I(s)$ is the current along the wire axis and $q(s)$ is the associated charge.

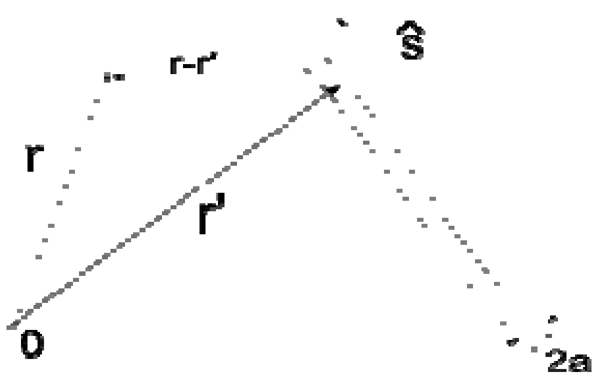

Figure 4: An arbitrarily oriented wire of radius 2a.

The wire is illuminated with an incident field $\vec{E}^{inc}$ and as a result produces a scattered field $\vec{E}^{s}$ arising from the induced current. Applying the boundary condition on the surface of a perfect conductor that the tangential component of the total electric field must vanish yields:

$$\left(\vec{E}^{inc} + \vec{E}^{s}\right)\cdot \hat{s} = \vec{0} \tag{21}$$

The scattered field can be written in terms of vector and scalar potentials as

$$\vec{E}^{s} = -j\omega\vec{A} - \nabla\Phi \tag{22}$$

Substituting Eq. (22) into Eq. (21) gives

$$-\vec{E}^{inc}\cdot\hat{s} = -j\omega\,\vec{A}\cdot\hat{s} - \nabla\Phi\cdot\hat{s} \tag{23}$$

The substitution of Equations (16) and (17) into Eq (23) yields an integral equation which can be solved numerically via the method of moments [6]. The wire is subdivided into $N+1$ segments, as shown in Figure 5.

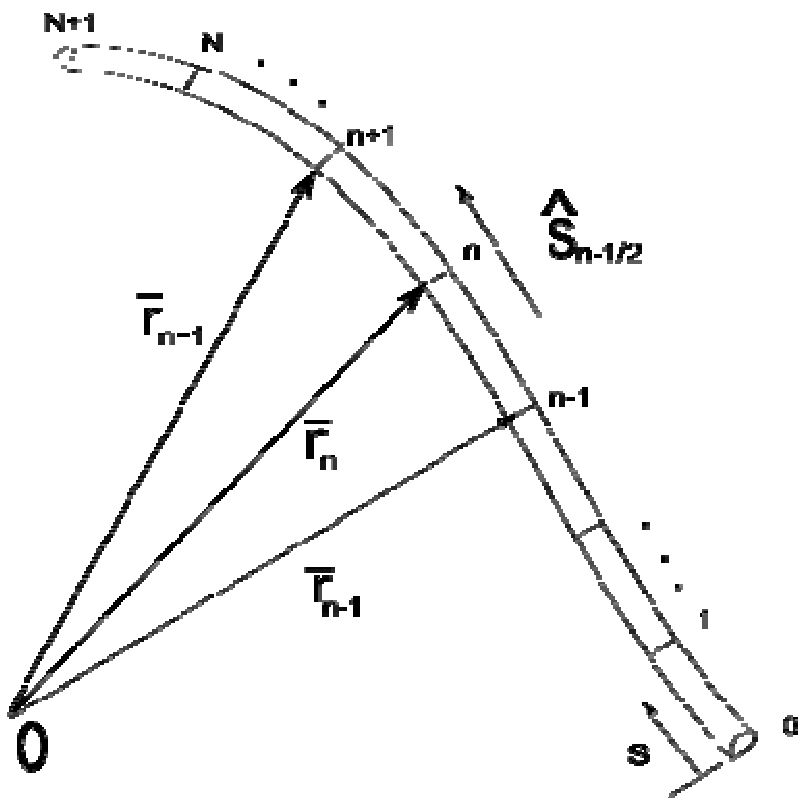

Figure 5: Arbitrarily oriented wire antenna with segmentation scheme.

The current and charge are expanded in terms of pulse basis functions. Note that the current and charge pulses are off by half a pulse width. For the current there is a half pulse of zero width on each end of the wire. This is not the case for the charge pulses which span the entire wire length. The current expansion can be written as

$$I(s) = \sum_{n=1}^{N} I_n P_n(s) \tag{24}$$

where the pulse function is defined as

$$P_n(s) = \begin{cases} 1, & s_{n-1/2} < s < s_{n+1/2} \\ 0, & otherwise \end{cases} \tag{25}$$

The variable s_n represents the arc length to the end of segment n measured from one end of the wire. The position vector $\vec{r}_n$ locates the end of wire segment n. The unit vector $\hat{s}_{n+1/2}$ is parallel to the wire axis on segment $n+1$ and defined as:

$$\hat{s}_{n+1/2} = \frac{\vec{r}_{n+1} - \vec{r}_n}{\left|\vec{r}_{n+1} - \vec{r}_n\right|} \tag{26}$$

Testing the integral equation in (23) with pulse functions yields a system of linear equations defined by

$$[Z_{mn}][I_n] = [V_m] \tag{27}$$

where

$$Z_{mn} = \frac{-1}{j4\pi\omega\varepsilon}\left[\begin{array}{l} k^2(\vec{r}_{m=1/2} - \vec{r}_{m-1/2}) \cdot (\hat{s}_{n+1/2}\Psi_{m,n,n+1/2} + \hat{s}_{n-1/2}\Psi_{m,n-1/2,n}) - \dfrac{\Psi_{m+1/2,n,n+1}}{s_{n+1} - s_n} + \dfrac{\Psi_{m+1/2,n-1,n}}{s_n - s_{n-1}} \\ + \dfrac{\Psi_{m-1/2,n,n+1}}{s_{n+1} - s_n} - \dfrac{\Psi_{m-1/2,n-1,n}}{s_n - s_{n-1}} \end{array}\right]$$

$$V_m = \vec{E}^{inc}(s_m) \cdot (\vec{r}_{m+1/2} - \vec{r}_{m-1/2})$$

$$\Psi_{m,u,v} = \int_{s_u}^{s_v} k(s_m - s')\, ds'$$

$$\vec{r}_{n+1/2} = \frac{\vec{r}_{n+1} + \vec{r}_n}{2}$$

$[Z_{mn}]$ is a square matrix with $m,n=1,2,...N$. $[I_n]$ and $[V_m]$ are column vectors of length N. The column vector $[V_m]$ represents an applied voltage at the location of the antenna feed point. For an antenna that is fed at the center with V volts, all the elements of $[V_m]$ are set equal to zero except the location that matches with the feed segment (the middle segment for the center-fed case).

Near Field Computation

The electric near field and the magnetic near field can be calculated using the current distribution obtained from the numerical procedure outlined earlier. The method is based on the work by Adams [7], [8]. To compute the electric field at a given point in the near field, a small (testing) thin wire dipole of length Δl is placed at the point with its axis parallel to the vector component of interest. An additional expansion function is assumed over this test dipole so that the total number of unknowns is $(N+1)$. If the test dipole is open circuited, then $I_{N+1}=0$ and the open circuit voltage is given by

$$V_{N+1}=\sum_{j=1}^{N} Z_{N+1,j}\, I_j \tag{28}$$

The electric field along the direction $\hat{l}$ is now given by

$$\vec{E}\cdot\hat{l}=-\frac{V_{N+1}}{\Delta l} \tag{29}$$

This process of placing the test dipole at the location of the near field point is repeated for each component (E_x, E_y, E_z) as well as for each near field point. The average value of the electric field is given by

$$E_{avg}=\left[\frac{1}{2}(E_x{}^2+E_y{}^2+E_z{}^2)\right]^{1/2} \tag{30}$$

and this is a conservative estimate of the maximum value. The maximum or peak value is given by

$$E_{peak}=\left[\frac{1}{2}(E_x{}^2+E_y{}^2+E_z{}^2)+\frac{1}{2}(A^2+B^2)^{1/2}\right]^{1/2} \tag{31}$$

where

$$A = E_x^2 \cos(2\theta_x) + E_y^2 \cos(2\theta_y) + E_z^2 \cos(2\theta_z)$$

$$B = E_x^2 \sin(2\theta_x) + E_y^2 \sin(2\theta_y) + E_z^2 \sin(2\theta_z)$$

and $\theta_x, \theta_y, \theta_z$ are the phase angles for the x, y, z components. The near magnetic field is calculated in a similar way as the electric field in terms of placing the test dipole and the computation is done using the vector potential. The magnetic field $\vec{H}$ can be computed from the vector potential $\vec{A}$ as

$$\vec{H} = \frac{1}{\mu}\nabla \times \vec{A} = \frac{1}{\mu}\left(\frac{\partial A_z}{\partial y} - \frac{\partial A_y}{\partial z}\right)\hat{x} + \frac{1}{\mu}\left(\frac{\partial A_x}{\partial z} - \frac{\partial A_z}{\partial x}\right)\hat{y} + \frac{1}{\mu}\left(\frac{\partial A_y}{\partial x} - \frac{\partial A_x}{\partial y}\right)\hat{z} \tag{32}$$

Where $\hat{x}, \hat{y}, \hat{z}$ are the unit vectors along the x, y, z coordinate axes, respectively. If the test dipole is short enough such that the fields vary smoothly over its' length then the partial derivatives in Equation (32) can be replaced by finite differences:

$$\vec{H} = \frac{1}{\mu}\left(\frac{\Delta A_z}{\Delta y} - \frac{\Delta A_y}{\Delta z}\right)\hat{x} + \frac{1}{\mu}\left(\frac{\Delta A_x}{\Delta z} - \frac{\Delta A_z}{\Delta x}\right)\hat{y} + \frac{1}{\mu}\left(\frac{\Delta A_y}{\Delta x} - \frac{\Delta A_x}{\Delta y}\right)\hat{z} \tag{33}$$

For example, $\Delta A_z / \Delta y$ is the change in the z component of the vector potential along a y directed test dipole of length Δy located at the near field point. The average and peak values of the magnetic field are computed using similar expressions as given for the electric field in Equations (30) and (31) with E replaced by H.

5.0 RESULTS AND DISCUSSION

In this section, numerical results on the near fields for a thin wire antenna are presented. The wire antenna is symmetrically located with its orientation in the z direction at $x = 0$, $y = 0$, as shown in Figure 6, and is center fed by a voltage of 1 volt at a frequency of 300 MHz. The antenna is sub-divided into $N+1$ segments, as shown in Figure 5, where N represents the number of pulse basis functions employed for the current distribution on the wire. Figure 7 shows the current distribution on a center-fed, half-wavelength dipole antenna of radius 0.005λ, number of pulses (unknowns) $N = 31$.

The current distribution is utilized in calculating the near fields using the formulation outlined in the previous section. A test dipole of length $\Delta l = 0.001\lambda$ in Equation (29) is used. Figures 8 and 9 show the computed near electric fields, E_z (z-component of Electric Field) and E_ρ (ρ-component of Electric Field), respectively, for the half-wavelength dipole as a function of z/λ for different values of radial distance ρ/λ. It can be seen from these figures that the radial component E_ρ has peaks at the gap ($z = 0$) and much higher peaks at the end of the dipole $(z/\lambda = 0.25)$. The tangential component of the electric field E_z is relatively small except in the gap region and near the end of the dipole antenna. Figure 10 shows the associated ϕ component of the magnetic field H_ϕ for this antenna configuration. Figures 11 and 12 show the computed near electric fields, E_z and E_ρ, respectively, for a 0.4484λ dipole as a function of z/λ for different values of radial distance ρ/λ. A copy of the computer code (developed in MATLAB) used to generate the result in Figure 11 is provided in Appendix I. Figures 13 and 14, the results obtained in this work for E_z and E_ρ, respectively, for the 0.4484λ dipole for ρ/λ =0.03 are compared with those obtained by Adams [8]. The comparison with published results is good, thereby, providing validity to the near field computation. The results for the 0.5λ dipole presented in Figures 8 and 9 also followed closely with published work of Adams [7]. The impedance and power density for the 0.5λ dipole are shown in Figures 15 and 16, respectively. The wave impedance in Figure 15 approaches the free space value of 377 ohms as ρ approaches the far field distance, r_{ff}, of 0.5λ ($r_{ff} = 2D^2/\lambda$, where $D = \lambda/2$ is the dimension of the antenna). It is interesting to notice that the impedance graph in Figure 15, for the case of $z/\lambda = 0.25$, does not seem to follow the trend of lower impedance values with increasing values of z/λ. A reasonable explanation for this case is that the electric field close to the tip of the antenna is very large, as seen from Figure 8, giving rise to large values of wave impedance.

6.0 CONCLUSIONS

The near field and far field regions are identified in terms of the antenna dimension. The near field of a thin wire antenna is computed for a half wave dipole. The method is applicable to any thin wire antenna as long as the wire radius is small compared to the wavelength, typically for radius $a \leq 0.001\lambda$. It is noted that the electric field variation in the near field is quite different than the traditional far field behavior. The electric field amplitude has peaks at certain locations which give rise to larger power density than conventionally expected. As the electric field undergoes through sharp peaks in the near field, the power density also shows a peaking behavior before following the far field trend. The wave impedance in the near field also undergoes sharp variations with distance from the antenna and approaches the free space value as the far field region is approached. The numerical model accurately characterizes the near field as the computed results are compared with results given in the literature. The model will therefore provide accurate estimation of near field so that radiation safety guidelines can be appropriately defined.

7.0 RECOMMENDATIONS

The present work modeled the near field of a thin wire antenna. The near field data from this work can now be imported as an input to the problem of computing the heating effects in a dielectric model of the human body. It is also recommended to model the near field of other antenna geometries such as a parabolic reflector antenna.

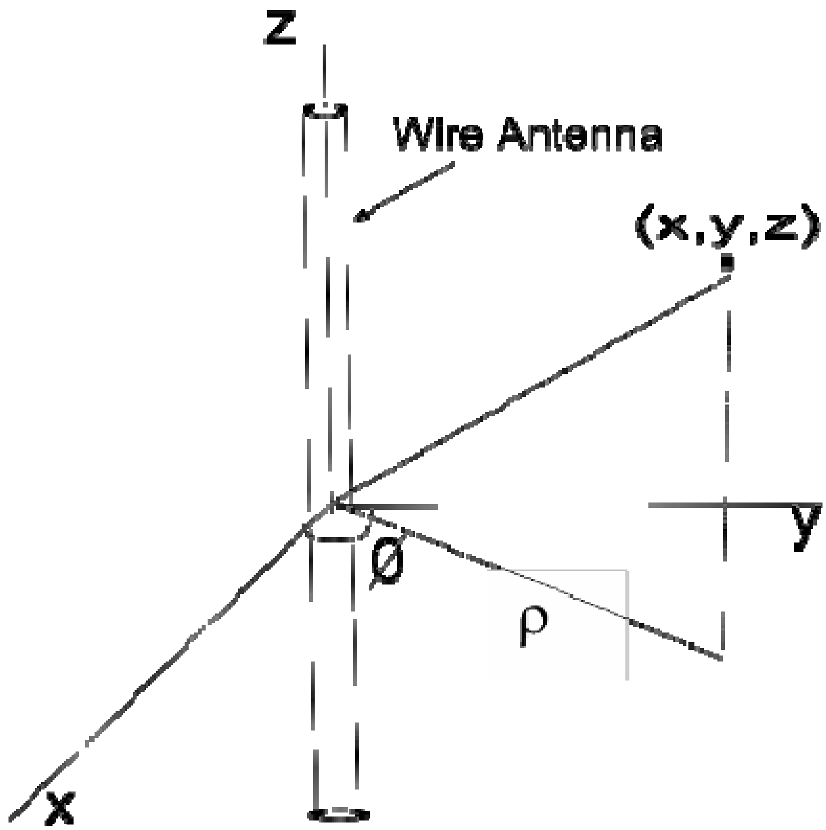

Figure 6: Wire antenna oriented symmetrically along the z-axis with field point (x, y, z).

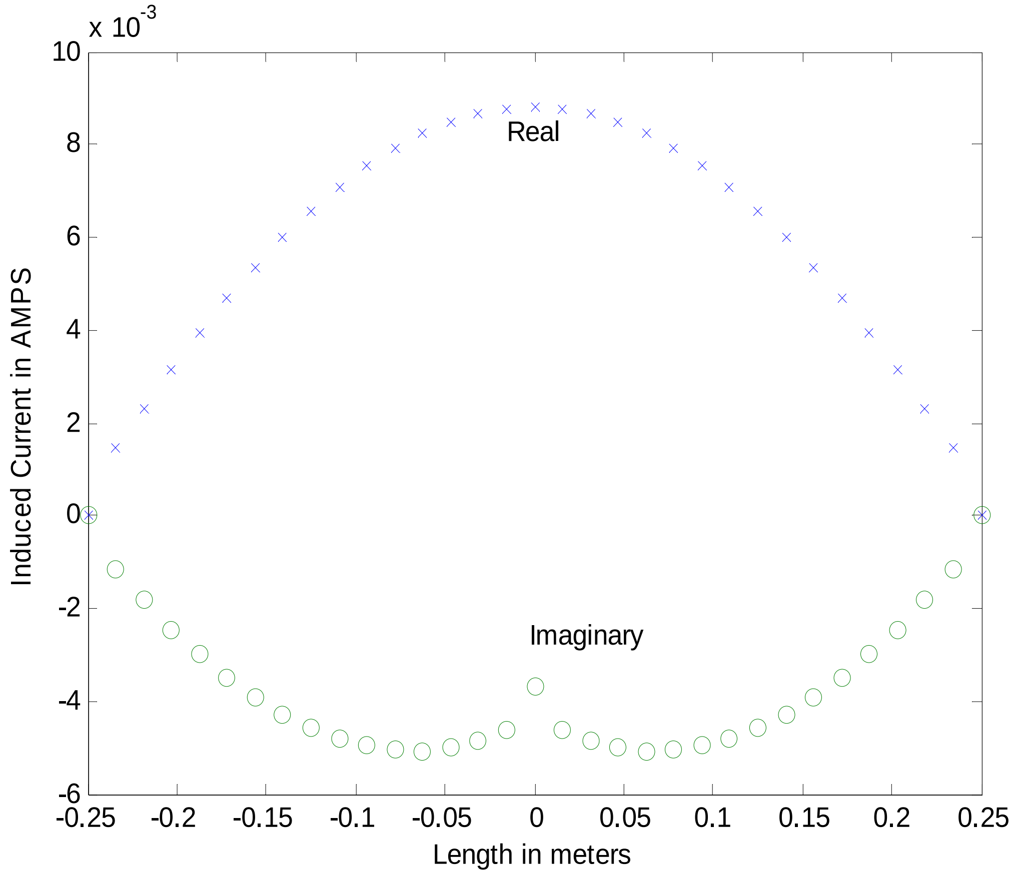

Figure 7: Current distribution on a center-fed, half-wavelength dipole (length = 0.5λ, radius = 0.005λ, frequency = 300 MHz).

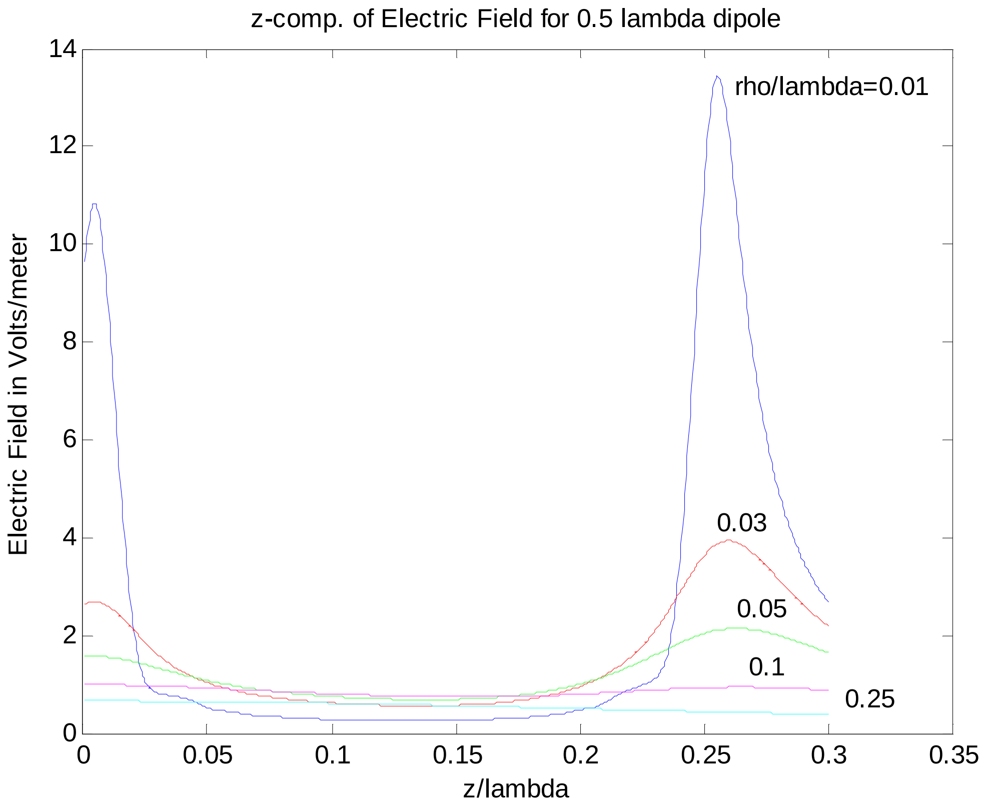

Figure 8: Near field E_z (z-component of Electric Field) of center-fed dipole antenna (length = 0.5 λ and radius = 0.005 λ).

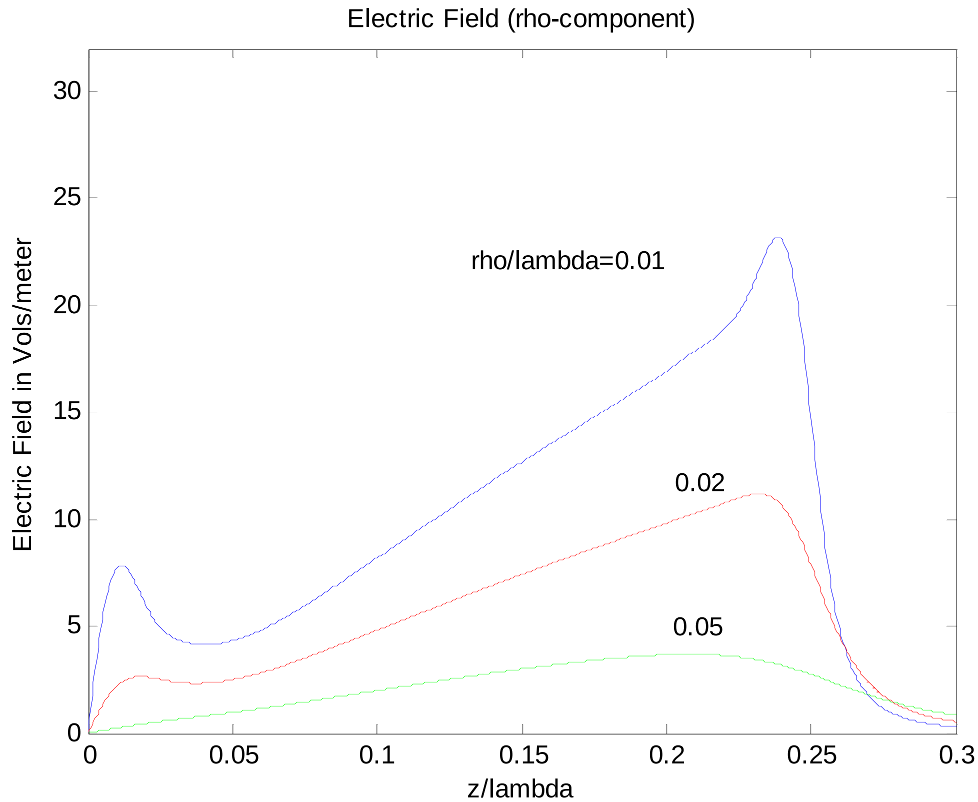

Figure 9: Near field E_ρ (ρ -component of Electric Field) of center-fed dipole antenna (length = 0.5 λ and radius = 0.005 λ).

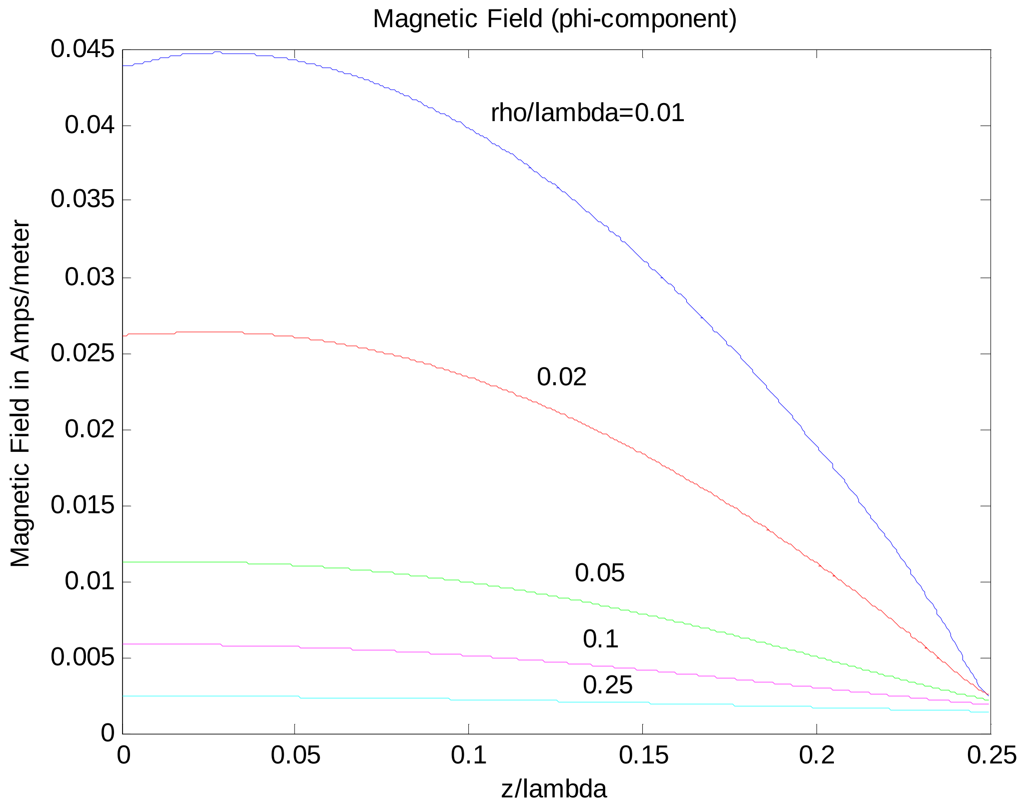

Figure 10: Near field H_ϕ (ϕ-component of Magnetic Field) of center-fed dipole antenna (length = 0.5 λ and radius = 0.005 λ).

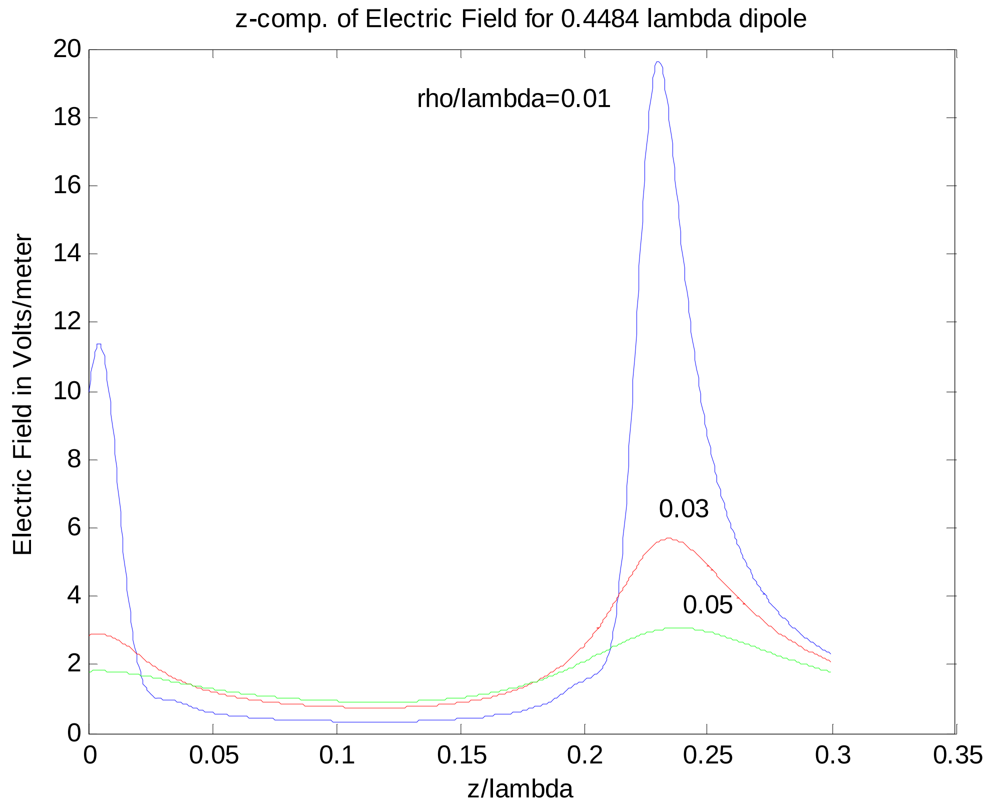

Figure 11: Near field E_z (z -component of Electric Field) of center-fed dipole antenna (length = 0.4484 λ and radius = 0.00503 λ).

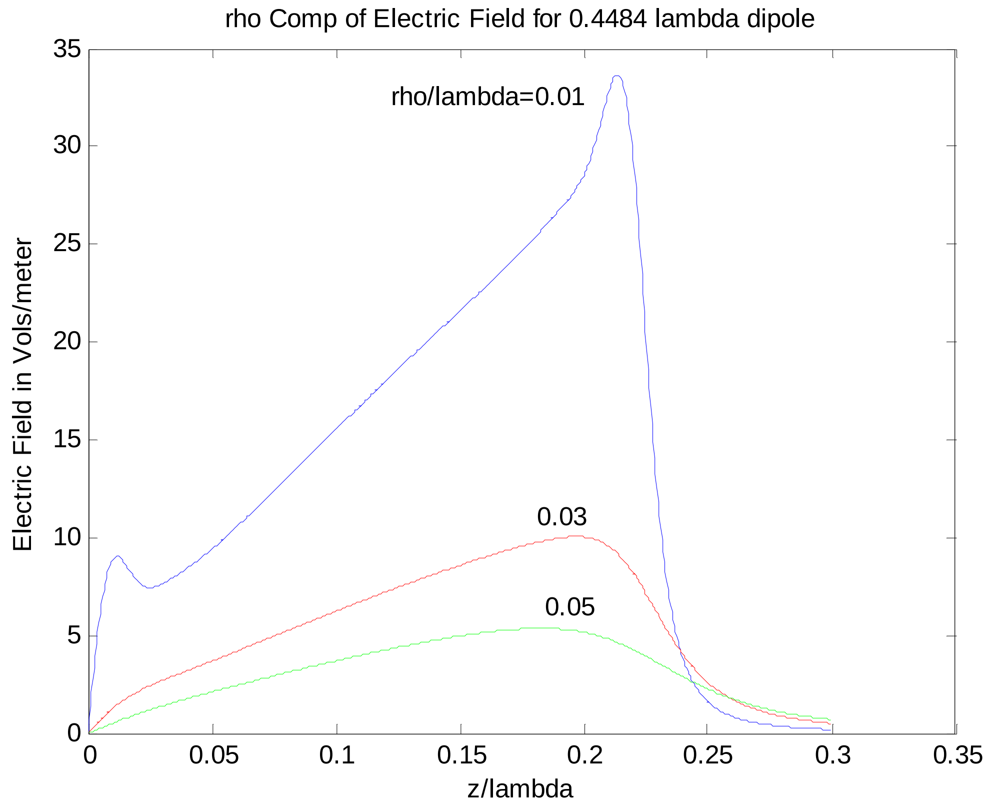

Figure 12: Near field E_ρ (ρ-component of Electric Field) of center-fed dipole antenna (length = 0.4484 λ and radius = 0.00503 λ).

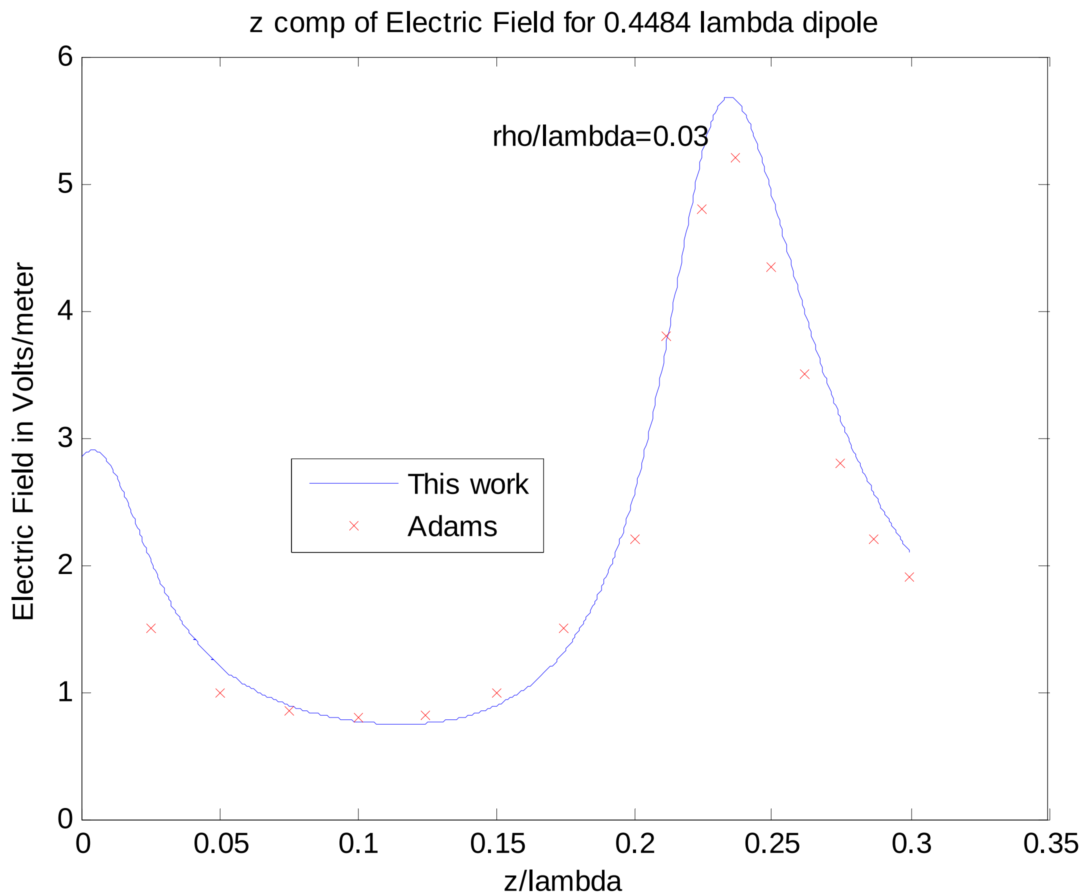

Figure 13: Near field E_z (z -component of Electric Field) of center-fed dipole antenna (length = 0.4484 λ and radius = 0.00503 λ).

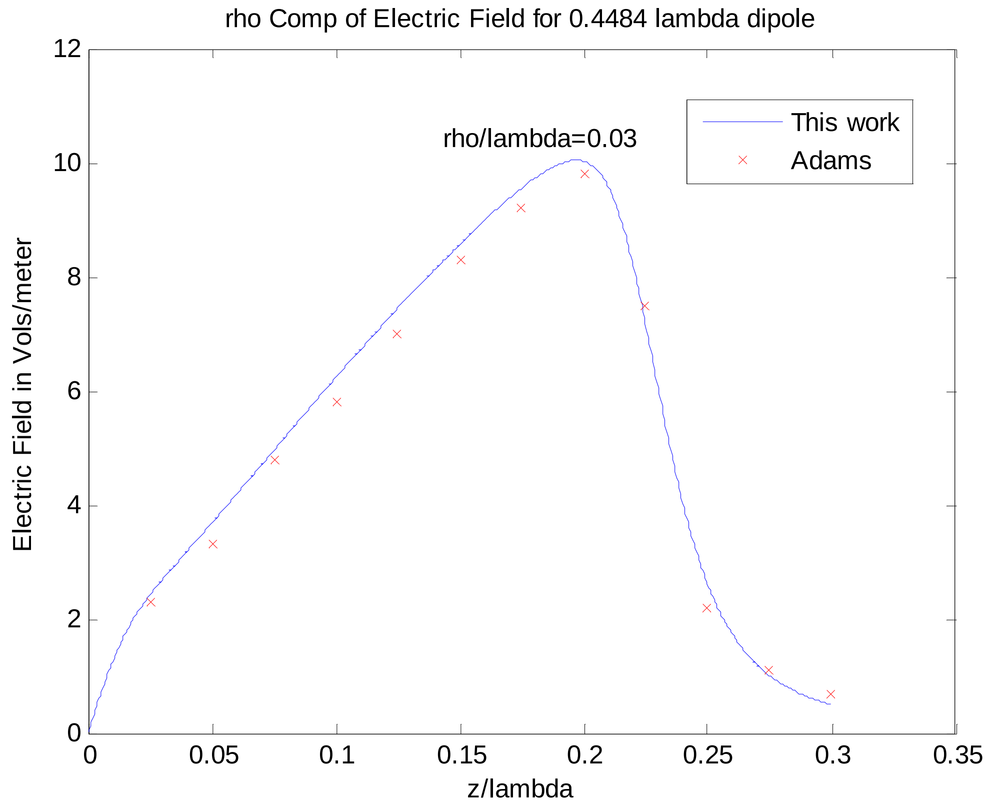

Figure 14: Near field E_ρ (ρ -component of Electric Field) of center-fed dipole antenna (length = 0.4484 λ and radius = 0.00503 λ).

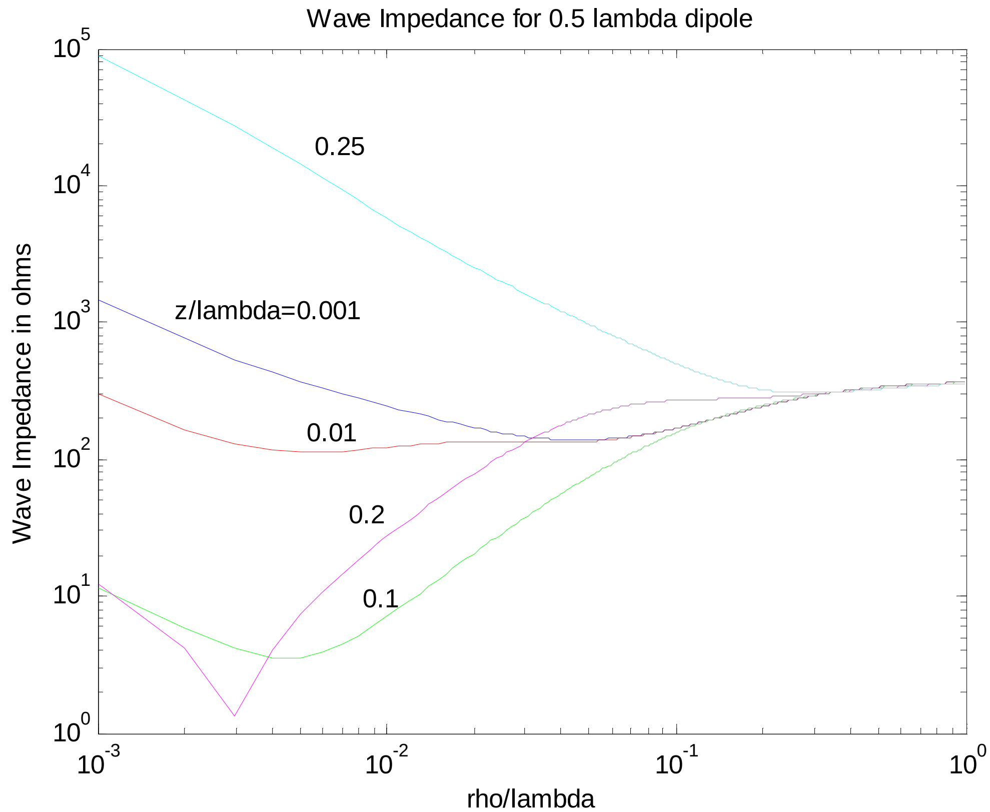

Figure 15: Wave Impedance for center-fed dipole (length = 0.5 λ and radius = 0.005 λ).

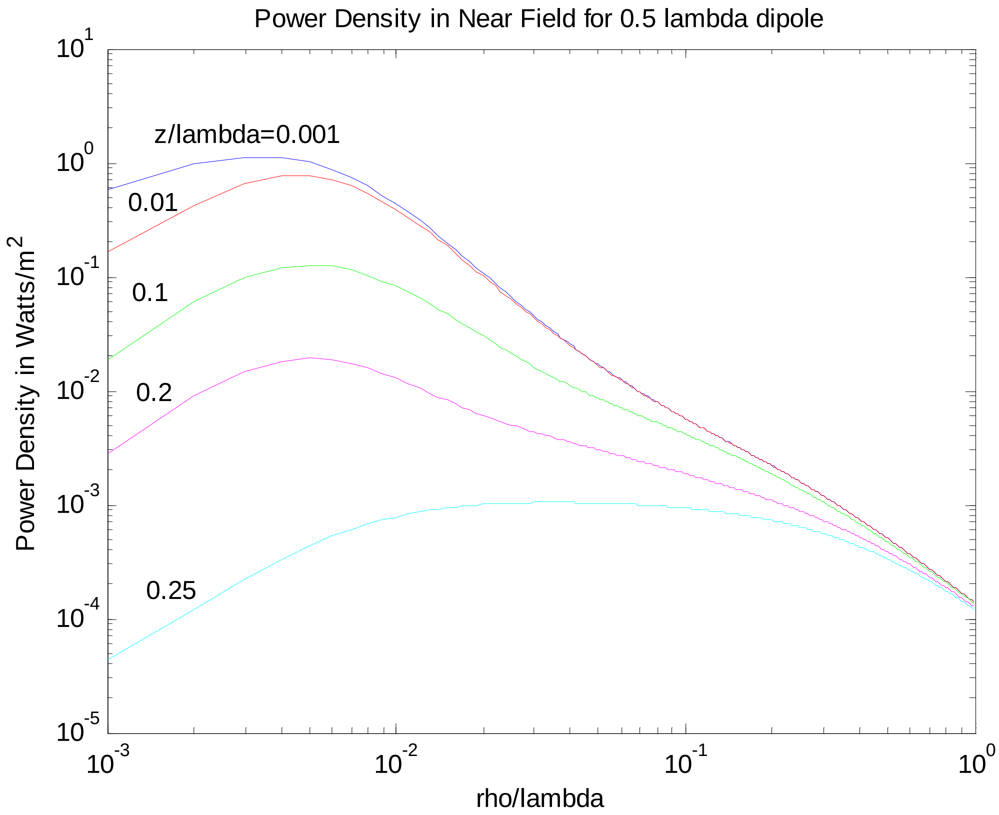

Figure 16: Power density for center-fed dipole (length = 0.5 λ and radius = 0.005 λ).

REFERENCES

1. FCC, Guidelines for Evaluating the Environmental Effects of Radiofrequency Radiation ET Docket No. 93-62, 1996.
2. W. W. Mumford, “Some technical aspects of microwave radiation hazards”, Proc. IRE, 1961, pp. 427-447.
3. Electromagnetic Radiation Hazards, TO 31Z-10-4, (ARMY) FM 11-490-30, May 25, 1989.
4. W. L. Stutzman and G. A. Thiele, Antenna Theory and Design, John Wiley & Sons, New York, 1981, pp. 19-24.
5. V. Jamnejad, “A study of effect of element pointing error on power density in near field of reflector arrays”, IEEE Conference on Aerospace, March 2005, pp. 1158-1175.
6. R. F. Harrington, R. Mittra and C. M. Butler, Lecture Notes for Short Course on Computational Methods in Electromagnetics, St. Cloud, Fl, 1980.
7. T. Adams, B.J. Strait, D. E. Warren, D-C Kuo and T. E. Baldwin, “Near fields of wire antennas by matrix methods”, IEEE Trans. Antennas & Propagation, vol. AP-21, no. 5, September 1973, pp. 602-610.
8. T. Adams, T. E. Baldwin and D. E. Warren, “Near fields of thin-wire antennas – computation and experiment”, IEEE Trans. Electromagnetic Compatibility, vol. EMC-20, no. 1, February 1978, pp. 259-266.

APPENDIX I : MATLAB CODE FOR ANTENNA NEAR FIELD

```
% z-comp of Electric Field (Near Field Calculation for a Wire
%Antenna) for near field calculation      August, 2007

clear all

%******************* INPUT    ******************************
% Variables with asterik (*) on the comment on the right side are INPUT
% VARIABLES

nunkns=31;             % ********  Number of Unknowns (for current) on
the Antenna
nunkns2=nunkns+2;
freq=300*10^6;    % *******************   Frequency (Hz)
vel=3*10^8;       % velocity of light in free space
omega=2*pi*freq;  % angular frequency (rad/sec)
wk=omega/vel;     % propagation constant (2*pi/lambda)
wavelength=vel/freq;  % wavelength (m)
length=0.2242*wavelength;    % ******************  Half dipole length
(in lambda)
dlength=2*length;
rad=0.005*wavelength;     % ********************  Radius of Dipole (in
lambda)
waveimp=377;                % **********  Wave Impedance in free space
(ohms)
eps=1/(36*pi*10^9);        % **********  Free space permittivity (F/m)
zg=0;                      % *********  Feed point of the antenna (zg=0
for Center-fed)
delta=2*length/(nunkns+1);  % Antenna segment length (2*L/(N+1))

  %   Grid points (x,y,z) where near field needs to be computed
dx=0;
dy=0;
dz=0.001;
ndx=1;
ndy=1;
ndz=300;
xstart=0.0*wavelength;
ystart_array(1)=0.01;
ystart_array(2)=0.03;
ystart_array(3)=0.05;
zstart=0.001*wavelength;

% ****** For Antenna case, the Dipole is Center-fed with 1 Volt ******
%              Forcing Function  "vmvector"  is Unity at feedpoint

for p=1:nunkns
```

```
    matchpnt=((nunkns-1)/2)+1;
   if p==matchpnt
      vmvector(p,1)=1.0;   % *******  Antenna feed voltage is 1 volt
   else
     vmvector(p,1)=0;
   end
end

% ************************* End of Input Data*******************

% The array rx,ry,rz gives the x,y,z components of wire segment end
points

for nn=1:nunkns2
    rx(nn)=0.0;
    ry(nn)=0.0;
    rz(nn)=-length+delta*(nn-1);
end

% Calculation of the Impedance Matrix "zmatrix"

 factor=-1/(j*4*pi*omega*eps);
for m=1:nunkns
    mp1=m+1;
    [rx1,ry1,rz1]= rmhvector(rx,ry,rz,mp1);
    [rx2,ry2,rz2]= rmhvector(rx,ry,rz,m);
    diffx=rx1-rx2;
    diffy=ry1-ry2;
    diffz=rz1-rz2;
   for n=1:nunkns
       np1=n+1;

       % Contribution due to vector potential

       psi1=vecpot(rx,ry,rz,wk,rad,mp1,np1, 0.5);
       psi2=vecpot(rx,ry,rz,wk,rad,mp1,np1,-0.5);

       %Contribution due to scalar potential

       psi3=scalarpot(rx,ry,rz,wk,rad,mp1,+0.5,np1,np1+1);
       psi4=scalarpot(rx,ry,rz,wk,rad,mp1,+0.5,np1-1,np1);
       psi5=scalarpot(rx,ry,rz,wk,rad,mp1,-0.5,np1,np1+1);
       psi6=scalarpot(rx,ry,rz,wk,rad,mp1,-0.5,np1-1,np1);

       % S unit vectors
       [sx1,sy1,sz1,rmag]=sunit(rx,ry,rz,np1);
       [sx2,sy2,sz2,rmag]=sunit(rx,ry,rz,n);

       % Dot products
       dot1=psi1*(diffx*sx1+diffy*sy1+diffz*sz1);
```

```
        dot2=psi2*(diffx*sx2+diffy*sy2+diffz*sz2);
        dotprod=wk^2*(dot1+dot2);

        zmatrix(m,n)=factor*(dotprod-psi3/delta+psi4/delta+psi5/delta-
psi6/delta);
   end
end


  %      SOLUTION BY MATRIX INVERSION

  solvector=inv(zmatrix)*vmvector; % solvector is the solution vector
%with current on the antenna


  %     Plot the Current Distribution on the Wire Antenna

   rsolvec=real(solvector);
   isolvec=imag(solvector);
   for ip=1:nunkns
       rrealpart(ip)=rsolvec(ip);
       iimagpart(ip)=isolvec(ip);
       zpart(ip)=rz(ip);
   end

  for ipp=1:nunkns2
      if ipp==1
        realpart(ipp)=0;
       imagpart(ipp)=0;
   elseif ipp==nunkns2
       realpart(ipp)=0;
       imagpart(ipp)=0;
   else
       realpart(ipp)=rrealpart(ipp-1);
       imagpart(ipp)=iimagpart(ipp-1);
   end
  end

   % If following three lines are commented out The Antenna Current is
%not plotted
          %  plot(rz,realpart,'x',rz,imagpart,'o')
          %  xlabel('Length in meters')
          %  ylabel('Induced Current in AMPS')



%    Near Field Computations
```

```
mp1=nunkns2+1;
for kk=1:3
 nfield_points=0;
 ystart=ystart_array(kk);
for i=1:ndx
    xd(i)=xstart+(i-1)*dx;
    xdi=xd(i);
    for j=1:ndy
        yd(j)=ystart+(j-1)*dy;
        ydj=yd(j);
        for k=1:ndz
            nfield_points=nfield_points+1;
            zd(k)=zstart+(k-1)*dz;
            zdk=zd(k);
      % efieldx,efieldy and efieldz are the x,y,z components of the
%Electric Field

      % **** NOTE ***** In this example only the z-comp of E-field is
%being computed
      % therefore, efieldx and efieldy are commented out

%efieldx=efieldnear(rx,ry,rz,xdi,ydj,zdk,solvector,wk,rad,factor,delta,
%wavelength,1,0,0,nunkns);

%efieldy=efieldnear(rx,ry,rz,xdi,ydj,zdk,solvector,wk,rad,factor,delta,
%wavelength,0,1,0,nunkns);

efieldz=efieldnear(rx,ry,rz,xdi,ydj,zdk,solvector,wk,rad,factor,delta,w
avelength,0,0,1,nunkns);

%       nearfield(kk,nfield_points)=abs(efieldx);  % if x-comp of near
%field is needed
%       nearfield(kk,nfield_points)=abs(efieldy);  % if y-comp of near
%field is needed
        nearfield(kk,nfield_points)=abs(efieldz);  % if z-comp of near
%field is needed

      end % loop over k  (z values)
    end % loop for j (y values)
  end % loop over i (x values)
  end %  loop over kk


  % Plot of Electric Field vs z/lambda for three values of rho/lambda

      plot(zd(:),nearfield(1,:),'b-')
      hold on
      plot(zd(:),nearfield(2,:),'r-')

      plot(zd(:),nearfield(3,:),'g-')
```

```
        title('z-comp. of Electric Field for 0.4484 lambda dipole')
        xlabel('z/lambda')
        ylabel('Electric Field in Volts/meter')
        gtext('rho/lambda=0.01')
        gtext('0.03')
        gtext('0.05')
        hold off

%%%%%%%%%%%%%%%%%%%%%%%%%%%%%%%%%%%%%%%%%%%%%%%%%%%%%%%%%%%%%%%%%%%

%%% FUNCTION USED IN THE MAIN PROGRAM

%%&&&&&&&&&&&&&&&&&&&&&&&&&&&&&&&&&&&&&&&&&&&&&&&&&&&&&&&&&&&&&&&

% &&&&&&&&&&   FUNCTION "rmhvector"   &&&&&&&&&&&&&&&

function[rmhx,rmhy,rmhz] = rmhvector(rx,ry,rz,p)
%Gives the x,y,z components of vector locating the mid-point of a
%segment
rmhx=(rx(p+1)+rx(p))/2;
rmhy=(ry(p+1)+ry(p))/2;
rmhz=(rz(p+1)+rz(p))/2;

% &&&&&&&&&&&&&  FUNCTION "sunit"    &&&&&&&&&&&&&&&&&&

function [snx,sny,snz,rmag] = sunit(rx,ry,rz,p)
%Gives x,y,z components of the unit vector,s_(p+1/2), on segment p to
%p+1
rx1=rx(p+1);
ry1=ry(p+1);
rz1=rz(p+1);
rx2=rx(p);
ry2=ry(p);
rz2=rz(p);
rmag=sqrt((rx1-rx2)^2+(ry1-ry2)^2+(rz1-rz2)^2);
snx=(rx1-rx2)/rmag;
sny=(ry1-ry2)/rmag;
snz=(rz1-rz2)/rmag;

% &&&&&&&&    FUNCTION  "scalarfun"    &&&&&&&&&&&&&&&


function psi=scalarfun(rx,ry,rz,wk,rad,m,n,del)
%psi function calculates the vector potential for H-field

rmx=rx(m);
rmy=ry(m);
rmz=rz(m);
```

```
% [rmx,rmy,rmz]=rmhvector(rx,ry,rz,m);

if del==0.5
    rnx=rx(n);
    rny=ry(n);
    rnz=rz(n);
    [sx1,sy1,sz1,rmag]=sunit(rx,ry,rz,n);
end
if del==-0.5
    [rnx,rny,rnz]=rmhvector(rx,ry,rz,n-1);
    [sx1,sy1,sz1,rmag]=sunit(rx,ry,rz,n-1);
end
delta2=rmag/2.0;
if m==n

    F=@(s) exp(-j*wk*sqrt((rmx-rnx-s*sx1).^2+(rmy-rny-s*sy1).^2+(rmz-
rnz-s*sz1).^2+rad.^2))./...
       sqrt((rmx-rnx-s*sx1).^2+(rmy-rny-s*sy1).^2+(rmz-rnz-
s*sz1).^2+rad.^2);
    psi=quad(F,0.0,delta2);
    % Self term calculation
else
    % Non-self term calculation (reduced kernel)

    F=@(s) exp(-j*wk*sqrt((rmx-rnx-s*sx1).^2+(rmy-rny-s*sy1).^2+(rmz-
rnz-s*sz1).^2+rad.^2))./...
       sqrt((rmx-rnx-s*sx1).^2+(rmy-rny-s*sy1).^2+(rmz-rnz-
s*sz1).^2+rad.^2);
    psi=quad(F,0.0,delta2);
end

%  &&&&&&&&&&  function  “scalarpot”  &&&&&&&&&&&&&&&&&&&&&&&


function psi=scalarpot(rx,ry,rz,wk,rad,m,del,n,q)
%psi function due to scalar potential
rnx=rx(n);
rny=ry(n);
rnz=rz(n);

rnx2=rx(q);
rny2=ry(q);
rnz2=rz(q);

[sx1,sy1,sz1,rmag]=sunit(rx,ry,rz,n);
if del==0.5
    [rmx,rmy,rmz]=rmhvector(rx,ry,rz,m);
end
if del==-0.5
    [rmx,rmy,rmz]=rmhvector(rx,ry,rz,m-1);
end
```

```
delta=rmag;
delta2=delta/2;
dist1=sqrt((rmx-rnx)^2+(rmy-rny)^2+(rmz-rnz)^2);
dist2=sqrt((rmx-rnx2)^2+(rmy-rny2)^2+(rmz-rnz2)^2);
if (dist1<delta)&(dist2<delta)
    % Self term calculation


      F=@(s) exp(-j*wk*sqrt((rmx-rnx-s*sx1).^2+(rmy-rny-s*sy1).^2+(rmz-
rnz-s*sz1).^2+rad.^2))./...
       sqrt((rmx-rnx-s*sx1).^2+(rmy-rny-s*sy1).^2+(rmz-rnz-
s*sz1).^2+rad.^2);
    psi=quad(F,0.0,delta);

else

    % Non-self term calculation - (Reduced kernel Approximation)

    F=@(s) exp(-j*wk*sqrt((rmx-rnx-s*sx1).^2+(rmy-rny-s*sy1).^2+(rmz-
rnz-s*sz1).^2+rad.^2))./...
       sqrt((rmx-rnx-s*sx1).^2+(rmy-rny-s*sy1).^2+(rmz-rnz-
s*sz1).^2+rad.^2);
    psi=quad(F,0.0,delta);

end



%   &&&&&&&&& FUNCTION “vecpot” &&&&&&&&&&&&&

function psi=vecpot(rx,ry,rz,wk,rad,m,n,del)
%psi function due to vector potential

rmx=rx(m);
rmy=ry(m);
rmz=rz(m);
if del==0.5
    rnx=rx(n);
    rny=ry(n);
    rnz=rz(n);
    [sx1,sy1,sz1,rmag]=sunit(rx,ry,rz,n);
end
if del==-0.5
    [rnx,rny,rnz]=rmhvector(rx,ry,rz,n-1);
    [sx1,sy1,sz1,rmag]=sunit(rx,ry,rz,n-1);
end
delta2=rmag/2.0;
if m==n
```

```
    F=@(s) exp(-j*wk*sqrt((rmx-rnx-s*sx1).^2+(rmy-rny-s*sy1).^2+(rmz-
rnz-s*sz1).^2+rad.^2))./...
       sqrt((rmx-rnx-s*sx1).^2+(rmy-rny-s*sy1).^2+(rmz-rnz-
s*sz1).^2+rad.^2);
    psi=quad(F,0.0,delta2);

    % Self term calculation



else
    % Non-self term calculation (reduced kernel)

    F=@(s) exp(-j*wk*sqrt((rmx-rnx-s*sx1).^2+(rmy-rny-s*sy1).^2+(rmz-
rnz-s*sz1).^2+rad.^2))./...
       sqrt((rmx-rnx-s*sx1).^2+(rmy-rny-s*sy1).^2+(rmz-rnz-
s*sz1).^2+rad.^2);
    psi=quad(F,0.0,delta2);
end

% &&&&&&&&&&&&&  FUNCTION “efield”  &&&&&&&&&&&&&&&&&&&&&&&

function efield =
efieldnear(rx,ry,rz,xdd,ydd,zdd,solvector,wk,rad,factor,delta,wavelengt
h,ix,iy,iz,nunkns)
% This function computes the near electric field E_x for ix=1,iy=0,iz=0
% This function computes the near electric field E_y for ix=0,iy=1,iz=0
% This function computes the near electric field E_z for ix=0,iy=0,iz=1

nunkns2=nunkns+2;
mp1=nunkns2+1;

if ix == 1

 %  ****  Compute x-Component of Electric Field  (E_x)  **********

    rx(mp1)=xdd-0.0005*wavelength;
    ry(mp1)=ydd;
    rz(mp1)=zdd;

    rx(mp1+1)=xdd;
    ry(mp1+1)=ydd;
    rz(mp1+1)=zdd;

    rx(mp1+2)=xdd+0.0005*wavelength;
    ry(mp1+2)=ydd;
    rz(mp1+2)=zdd;

elseif iy == 1
```

```
     %  *** Compute y-Component of Electric Field  (E_y)  **********

    rx(mp1)=xdd;
    ry(mp1)=ydd-0.0005*wavelength;
    rz(mp1)=zdd;


    rx(mp1+1)=xdd;
    ry(mp1+1)=ydd;
    rz(mp1+1)=zdd;

    rx(mp1+2)=xdd;
    ry(mp1+2)=ydd+0.0005*wavelength;
    rz(mp1+2)=zdd;

   else

    rx(mp1)=xdd;
    ry(mp1)=ydd;
    rz(mp1)=zdd-0.0005*wavelength;


    rx(mp1+1)=xdd;
    ry(mp1+1)=ydd;
    rz(mp1+1)=zdd;

    rx(mp1+2)=xdd;
    ry(mp1+2)=ydd;
    rz(mp1+2)=zdd+0.0005*wavelength;
end
        %  ****Compute z-Component of Electric Field  (E_z)  **********


    [rx1,ry1,rz1]= rmhvector(rx,ry,rz,mp1+1);
    [rx2,ry2,rz2]= rmhvector(rx,ry,rz,mp1);

    diffx=rx1-rx2;
    diffy=ry1-ry2;
    diffz=rz1-rz2;

    esum=0.0;

    for n=1:nunkns
       np1=n+1;

       % Contribution due to vector potential

       psi1=vecpot(rx,ry,rz,wk,rad,mp1+1,np1, 0.5);
```

```
        psi2=vecpot(rx,ry,rz,wk,rad,mp1+1,np1,-0.5);

        %Contribution due to scalar potential

        psi3=scalarpot(rx,ry,rz,wk,rad,mp1+1,+0.5,np1,np1+1);
        psi4=scalarpot(rx,ry,rz,wk,rad,mp1+1,+0.5,np1-1,np1);
        psi5=scalarpot(rx,ry,rz,wk,rad,mp1+1,-0.5,np1,np1+1);
        psi6=scalarpot(rx,ry,rz,wk,rad,mp1+1,-0.5,np1-1,np1);

        % S unit vectors
        [sx1,sy1,sz1,rmag]=sunit(rx,ry,rz,np1);
        [sx2,sy2,sz2,rmag]=sunit(rx,ry,rz,n);

        % Dot products
        dot1=psi1*(diffx*sx1+diffy*sy1+diffz*sz1);
        dot2=psi2*(diffx*sx2+diffy*sy2+diffz*sz2);
        dotprod=wk^2*(dot1+dot2);

        matrix=factor*(dotprod-psi3/delta+psi4/delta+psi5/delta-
psi6/delta);
        esum=esum+matrix*solvector(n);
    end % Loop over n; E_x Component

      efield = -esum/0.001/sqrt(2);  % x-comp of Electric Field
```